INTRINSIC QUANTUM THERMODYNAMIC PREDICTION OF THE NON-EQUILIBRIUM ATOMISTIC-LEVEL BEHAVIOUR OF CHEMICALLY REACTIVE SYSTEMS

Omar Al-Abbasi*, Gian Paolo Beretta°, Michael R. von Spakovsky*

* Mechanical Engineering Department, Virginia Tech, Blacksburg, Virginia, 24061, USA
° Department of Mechanical and Industrial Engineering, Università di Brescia, Brescia, 25123, Italy

ABSTRACT

This paper presents an application of a fundamentally new approach called Intrinsic Quantum Thermodynamic (IQT) to the prediction of the kinetics of chemically reactive systems at small scales. The IQT framework satisfies the laws of quantum mechanics as well as thermodynamics and provides an alternative, comprehensive, and reasonable means for modeling non-equilibrium processes even far from equilibrium. It does so without the need for any of the a priori limiting assumptions common to most conventional methods in the literature such as that of stable equilibrium via a specific choice of temperature or of pseudo-equilibrium between reactants and activated complex. The IQT framework assumes time evolution along the steepest entropy ascent path in state space and is, in fact, able to predict a unique non-equilibrium path, which the system takes in relaxing from a state of non-equilibrium to that of stable equilibrium, and in so doing, dynamically provides a plausible complete picture of the changes occurring in key thermodynamic properties (e.g., the instantaneous species concentrations, entropy and entropy generation, reaction coordinate, chemical affinities, reaction rate, etc.) throughout the reaction process. In this paper, the IQT framework is applied to a chemically reactive system governed by the reaction mechanism

INTRODUCTION

This paper discusses the use of a relatively new theory known as intrinsic quantum thermodynamics (IQT) [1-4] to predict the reaction kinetics at atomistic levels of chemically reactive systems in the non-equilibrium realm. IQT has emerged over the last three decades as the theory that not only unifies two of the three theories of physical reality, namely, quantum mechanics (QM) and thermodynamics, but as well provides a physical basis for both the entropy and entropy production. The IQT framework is able to describe the evolution in state of a system undergoing a dissipative process based on the principle of steepest entropy ascent or locally maximal entropy generation [5]. The dynamical postulate of this theory was formulated originally to predict the evolution dynamics of closed, isolated systems composed of a single particle, an assembly of indistinguishable particles, or a field [6] or a set of distinguishable particles, fields, or some combination of these [7]. More recently some preliminary attempts have been made to extend the IQT equation of motion so as to model a larger class of systems, namely, those involving heat [8-10] and/or mass interactions [10].

The work presented in this paper demonstrates for the first time the use of the IQT framework to model the evolution in state of a chemically reactive system as its state relaxes to stable equilibrium. This framework brings a number of benefits to the field of reaction kinetics. Among these is the ability to predict a unique, non-equilibrium (kinetic), thermodynamic path, i.e., unique cloud of trajectories, which the state of the system follows in relaxing to stable equilibrium. As a consequence, the reaction rate kinetics at every instant of time is known as are the chemical affinities, the reaction coordinates, the direction of reaction, the activation energies, the entropy, the entropy production, etc. All is accomplished without any a priori limiting assumption of stable equilibrium via a specific choice of temperature nor of pseudo-equilibrium between reactant and activated complex. This is fundamentally different from all conventional methods (e.g., Transition State Theory [11,12], Trajectory Calculations [13], Quantum Scattering Theory [14, 15], etc.), which envision the reaction as a process driven only by collisions (i.e., the laws of mechanics, whether classical or quantum). In contrast, IQT envisions the same problem driven by both the laws of mechanics and thermodynamics. It is, thus, able to provide detailed information about the so-called state-to-state reaction channels and is not only able to predict the thermal reaction rate constant but its instantaneous details as well. As a consequence, this rate constant is transformed into a variable rate of the reaction process.

To illustrate the IQT approach, the

$$F + H_2 \Leftrightarrow FH + H \tag{1}$$

reaction mechanism, which for decades has been under intensive investigation both theoretically and experimentally [16,17], is used to benchmark the IQT results and illustrate the IQT reaction kinetics in the non-equilibrium realm.

IQT MODEL

The application of the general IQT framework for chemically reactive systems at small scales developed by Beretta and von Spakovsky [18] to the chemical kinetics of these systems is consistent with the idea put forward by Ziegler [19] concerning the thermodynamic consistency of the standard model of chemical kinetics. In modeling the non-equilibrium time evolution of state of these systems, both the system energy and particle number eigenvalue problems as well as the non-linear IQT equation of motion must be solved. The former establish the so-called energy and particle number eigenstructure of the system, i.e., the landscape of quantum eigenstates available for the system, while the latter determines the unique non-equilibrium thermodynamic path taken by the

system, showing how the density operator ρ, which represents the thermodynamic state of the system at every instant of time, evolves from a given initial non-equilibrium state to the corresponding stable chemical equilibrium state. For this framework, the thermodynamic system is defined as an isolated system consisting of *r* different reacting species contained in a tank.

In the present paper, only the principal IQT model equations are presented. For complete details of the model, the reader is referred to [18]. To begin with, the system energy and particle occupation number eigenvalue problems, which must be solved to establish the landscape of quantum eigenstates available for the system, are the following:

$$H\left|\xi_{sq_s}\right\rangle = E_{sq_s}\left|\xi_{sq_s}\right\rangle \quad s=1,\ldots,C \quad q_s=1,\ldots,L_s \tag{2}$$

where *H* is the system-level Hamiltonian, E_{sq_s} the system-level energy eigenvalue, ξ_{sq_s} the system-level eigenvector, *C* the number of subspaces of compatible compositions, and L_s the dimension of subspace *s*. The dimension of the overall Hilbert space $\mathscr{H}$ of the system is $L=\sum_{s=1}^{C}L_s$. A Hilbert as opposed to Fock space is assumed since the framework presented is based on the assumption that, consistent with the earlier assumption of an isolated system, the number of atoms is fixed (i.e., is conserved) and always known [18]. The corresponding system-level particle occupation number eigenvalue problem is expressed as

$$N_{A_i j_i}\left|\xi_{sq_s}\right\rangle = \alpha_{ij_i}^{sq_s}\left|\xi_{sq_s}\right\rangle \quad \begin{array}{l} s=1,\ldots,C \quad q_s=1,\ldots,L_s \\ i=1,\ldots,r \quad j_i=1,\ldots,M_i \end{array} \tag{3}$$

$$N_{A_i}=\sum_{j_i=1}^{M_i}N_{A_i j_i} \tag{4}$$

where A_i is the i^{th} species, N_{A_i} the A_i-particles number operator, $N_{A_i j_i}$ the A_i-particles-in-the-j_i^{th}-internal-level occupation number operator, and $\alpha_{ij_i}^{sq_s}$ the A_i-particles-in-the-j_i^{th}-internal-level eigenvalue for the q_s^{th} combination in the s^{th} compatible composition. M_i is the number of eigenvectors of the one-A_i-particle internal Hamiltonian operator associated with the internal degrees of freedom (i.e., vibrational, rotational, etc. energy levels).

Defining the Hilbert space and the set of eigenvectors that span that space requires that the initial amounts n_{ia} for each species A_i in the reacting mixture be related to the set of compatible amounts via the proportionality relations [20], namely,

$$n_{is}=n_{ia}+\sum_{l=1}^{\tau}\nu_{il}\varepsilon_{ls}=n_{ia}+\boldsymbol{\nu}_i\cdot\boldsymbol{\varepsilon}_s\geq 0 \tag{5}$$

where n_{is} is the eigenvalue of the amount of the A_i species for the subspace *s*, ν_{il} the stoichiometric coefficient for species A_i in reaction mechanism "*l*", $\boldsymbol{\nu}_i$ the set of stoichiometric coefficients for species A_i in each of the τ reaction mechanisms, ε_{ls} the eigenvalue of the reaction coordinate operator of reaction "*l*" that corresponds to the s^{th} compatible composition, and $\boldsymbol{\varepsilon}_s$ the set of reaction coordinate eigenvalues identifying the s^{th} compatible composition. This set of inequality equations determines the number of compatible solutions (i.e., subspaces *s*). Note that the n_{is} are related to the $\alpha_{ij_i}^{sq_s}$ via

$$n_{is}=\sum_{j_i}^{M_i}\alpha_{ij_i}^{sq_s} \quad \text{for every} \quad q_s=1,\ldots,L_s \tag{6}$$

Equations (2) and (3) are not solved directly due to their complexity but instead related to a set of one-particle eigenvalue problems, which can be solved. For details of how this is done, the reader is referred to [18]. The result is that, the one-particle A_i energy eigenvalues and eigenvectors for the internal degrees of freedom are made to correspond to the system-level ones via the following relations:

$$\left|\xi_{sq_s^{int}}^{int}\right\rangle=\bigotimes_{i=1}^{r}\left(\bigotimes_{j_i=1}^{M_i}\left|\varepsilon_{j_i}^{A_i}\right\rangle^{\otimes\alpha_{ij_i}^{sq_s^{int}}}\right) \tag{7}$$

$$E_{sq_s^{int}}^{int}=\sum_{i=1}^{r}\sum_{j_i=1}^{M_i}e_{j_i}^{A_i}\alpha_{ij_i}^{sq_s^{int}} \tag{8}$$

and for the translational degrees of freedom via the following:

$$\left|\xi_{sq_s^{tr}}^{tr}\right\rangle=T^{-1}\left(\bigotimes_{j_s=1}^{n_s}\left|\hat{\varepsilon}_{k_{sj_s}}^{sj_s}\right\rangle\right) \tag{9}$$

$$E_{sq_s^{tr}}^{tr}=e_{k_{s1}}^{s1}+\ldots+e_{k_{sj_s}}^{sj_s}+\ldots+e_{k_{sn_s}}^{sn_s} \tag{10}$$

where the $q_s^{tr}=\left(k_{s1},\ldots,k_{sj_s},\ldots,k_{sn_s}\right)$, each $k_{sj_s}=1,\ldots,K_{sj_s}$, and K_{sj_s} corresponds to some practical truncation of what is an infinite dimensional problem. In addition, T^{-1} in Eq. (9) signifies an inverse unitary transformation from the center-of-mass coordinate frame in which the one-particle translational eigenvalue problems are solved. The system-level energy eigenvalues and eigenvectors are now found from those for the various degrees of freedom via

$$\left|\xi_{sq_s}\right\rangle=\left|\xi_{sq_s^{tr}}^{tr}\right\rangle\otimes\left|\xi_{sq_s^{int}}^{int}\right\rangle \tag{11}$$

and $$E_{sq_s}=E_{sq_s^{tr}}^{tr}+E_{sq_s^{int}}^{int} \tag{12}$$

The system-level Hamiltonian is next constructed according to the following expression:

$$H=\sum_{s=1}^{C}\sum_{q_s=1}^{L_s}E_{sq_s}P_{\mathscr{H}_{sq_s}} \tag{13}$$

where the projector $P_{\mathscr{H}_{sq_s}}$ is given by

$$P_{\mathscr{H}_{sq_s}}=\left|\xi_{sq_s}\right\rangle\left\langle\xi_{sq_s}\right| \tag{14}$$

In a like manner, the particle number operator for each species is written as

$$N_{A_i}=\sum_{s=1}^{C}\sum_{j_i=1}^{M_i}\sum_{q_s=1}^{L_s}\alpha_{ij_i}^{sq_s}P_{\mathscr{H}_{sq_s}} \tag{15}$$

The preceding quantities provide the basis for determining the set of occupation probabilities y_{sq_s}, which correspond to the density operator ρ at any given instant of time and in turn are used to calculate the expectation values of properties or observables of interest. Thus,

$$y_{sq_s}=\mathrm{Tr}\left(\rho P_{\mathscr{H}_{sq_s}}\right)=\left\langle\xi_{sq_s}\left|\rho\right|\xi_{sq_s}\right\rangle \tag{16}$$

and the expectation energy of the system is given by

$$\langle H\rangle=\mathrm{Tr}\left(\rho H\right)=\sum_{s=1}^{C}\sum_{q_s=1}^{L_s}y_{sq_s}E_{sq_s} \tag{17}$$

The expectation value for the number of particles of species A_i is found from

$$\left\langle N_{A_i}\right\rangle=\sum_{j_i=1}^{M_i}\left\langle N_{A_i j_i}\right\rangle=\sum_{s=1}^{C}\sum_{q_s=1}^{L_s}y_{sq_s}\sum_{j_i=1}^{M_i}\alpha_{ij_i}^{sq_s} \tag{18}$$

while that for the reaction coordinate is given by

$$\langle\boldsymbol{\varepsilon}\rangle=\sum_{s=1}^{C}\boldsymbol{\varepsilon}_s\sum_{q_s=1}^{L_s}y_{sq_s} \tag{19}$$

or on a rate basis by

$$\left\langle \dot{\boldsymbol{\varepsilon}} \right\rangle = \sum_{s=1}^{C} \boldsymbol{\varepsilon}_s \sum_{k=1}^{L_s} \dot{y}_{sq_s} \tag{20}$$

Now, the IQT equation of motion governing the reaction kinetics for the system considered here is the following:

$$\frac{d\rho}{dt} = -\frac{i}{\hbar}[H,\rho] + \frac{1}{2k_B\tau}\{\Delta M,\rho\} \tag{21}$$

where the first term on the right governs the linear Hamiltonian dynamics of the state evolution and the second, the so-called dissipation term, the nonlinear non-Hamiltonian steepest-entropy-ascent dynamics. In this equation, τ is the internal-relaxation time for the dissipation, $\{\ \}$ the anti-commutator operator, k_B Boltzmann's constant, and $\Delta M = M - \langle M \rangle$ the deviation from the mean of the non-equilibrium Massieu operator defined as

$$M = S - H/\theta_H \tag{22}$$

where S and H are the entropy and Hamiltonian operators, respectively, and θ_H is a constant-energy, nonequilibrium temperature given in terms of the variance of the entropy and Hamiltonian operators by

$$\theta_H(\rho) = \langle \Delta H \Delta H \rangle / \langle \Delta S \Delta H \rangle \tag{23}$$

The entropy operator S is expressed by one of two equivalent forms, namely,

$$S = -k_B \ln(\rho + P_o) = -k_B B \ln \rho \tag{24}$$

with P_o and B, respectively, the projection operators onto the range and the kernel of ρ.

ONE-PARTICLE ENERGY EIGENVALUES

It is assumed that the reacting mixture considered here behaves as a Gibbs-Dalton mixture of ideal gases. For that reason, the energy eigenvalues for translation, vibration, and rotation for the species involved are given by a set of closed-form relations. For translation,

$$\varepsilon_k^{tr} = \frac{h^2}{8m}\left(\left(\frac{n_x}{L_x}\right)^2 + \left(\frac{n_y}{L_y}\right)^2 + \left(\frac{n_z}{L_z}\right)^2\right) \tag{25}$$

where ε_k^{tr} is the one-particle translational energy eigenvalue; h is Plank's constant; m is the mass of the particle; k=1,2,… is the principal quantum number; n_x, n_y and n_z are the quantum numbers in the x, y and z directions, respectively; and L_x, L_y, and L_z are the dimensions for the system volume in the x, y, and z directions, respectively.

For vibration, the expression is

$$\varepsilon_v^{vib} = v\left(v + \tfrac{1}{2}\right)\omega\hbar^2 \tag{26}$$

where v is the vibrational quantum number which takes values of v=0,1,2,…; ω is the vibrational frequency; and $\hbar$ Plank's modified constant. A wide range of wavenumbers from which ω can be calculated are reported in the literature [21, 22]. In the present paper, the wavenumber values used are 4401 cm^{-1} for H_2 and 4000 cm^{-1} for FH.

Finally, for rotation, the following expression is used:

$$\varepsilon_J^{rot} = \frac{J(J+1)\,\hbar^2}{2\mu r^2} \tag{27}$$

where J is the rotational quantum number that takes values of J=0,1,2,…; μ is the reduced mass; and r the distance between two atoms.

NUMERICAL APPROACH

For purposes of this paper and the preliminary comparisons given below, the system considered here initially consists of 1 particle of F and 1 of H_2 and is governed by the reaction mechanism of Eq. (1). The degrees of freedom for each of the molecules and atoms in the IQT model are given in Table 1.

To apply the IQT equation of motion to this IQT model, the density operator for an initial non-equilibrium state is required. Such a state far from equilibrium is found by first finding the density operator or matrix ρ^{pe} for a partially canonical state

Table 1. Quantum numbers considered for each of the molecules and atoms in the IQT model.

Species	Translational quantum nos.[a]	Vibrational quantum nos.	Rotational quantum nos.
F	k=1,...,400		
H_2	k=1,...,400	v=0	J=0,1
FH	k=1,...,400	v=0,1,2,3	J=0,1,...,7
H	k=1,...,400		

[a] Although the translational principal quantum number k varies here from 1 to 400 for each species, only a sampling (30) of these quantum numbers across this range is used for each species in the IQT model.

and then perturbing it. To determine ρ^{pe}, the following set of equations for the occupation probabilities y_j^{pe} must be solved:

$$y_j^{pe} = \frac{\delta_j\, e^{(-\beta E_j)}}{\sum_{k=1} \delta_k\, e^{(-\beta E_k)}} \tag{28}$$

subject to the constraints

$$Tr\left(\rho^{pe} H\right) = \sum_j y_j^{pe} E_j = \langle H \rangle \tag{29}$$

$$Tr\left(\rho^{pe} N_{A_i}\right) = \sum_j y_j^{pe} \left(n_j\right)_i = \left\langle N_{A_i} \right\rangle \quad i = 1,\ldots,r \tag{30}$$

The E_j in these equations are the system-level energy eigenvalues and the $(n_j)_i$ the system-level particle number eigenvalues for the i^{th} species. The values for the δ_j for each reactant species are set to either 0 or 1. As long as at least one of the δ_j has a value of 0, Eq. (28) describes the occupation probabilities for the density operator or matrix of a partially canonical state.

To find the initial non-equilibrium density operator or matrix, ρ^{pe} is perturbed as follows:

$$f_j = 1 - \lambda + \lambda \frac{y_j^{pe}}{y_j^{se}} \tag{31}$$

$$y_j = \frac{f_j\, y_j^{se}}{\sum_{i=1} f_i\, y_i^{se}} \tag{32}$$

where λ is an arbitrary perturbation parameter constrained by $0 < \lambda < 1$ and the y_j^{se} are the occupation probabilities for the stable equilibrium density matrix given by

$$y_j^{se} = e^{\left(\frac{-E_j}{k_b T}\right)} \Big/ \sum_{k=1} e^{\left(\frac{-E_k}{k_b T}\right)} \tag{33}$$

Here T is the stable equilibrium temperature.

Once the initial density operator or matrix is found, Eq. (21) is solved for the evolution in state of the system. This equation has been solved here using a forth order Runge–Kutta explicit scheme with the relative tolerance error set to 1e-5.

RESULTS AND DISCUSSION

Predicting the value of the entropy and the entropy generation at each instant of time are direct outcomes of the

IQT framework since the 1st and 2nd laws of thermodynamics are explicitly built into the equation of motion. Figures 1 and 2 show how both the entropy and the rate of entropy generation of the system evolve in time. A state of stable equilibrium is reached when the entropy plateaus out. In addition, the peak in the rate of entropy generation occurs quite early in the process and then quickly decreases as stable equilibrium is approached.

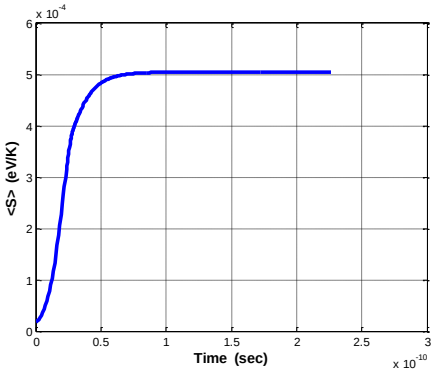

Figure 1. The instantaneous entropy of the reaction processing system.

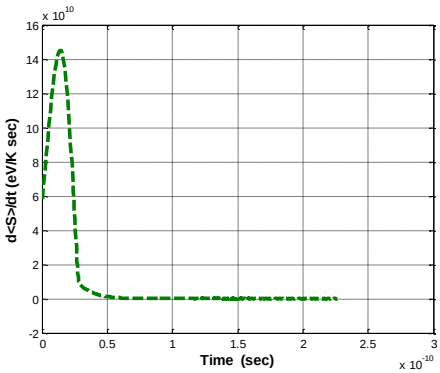

Figure 2. The instantaneous entropy generation during the reaction process.

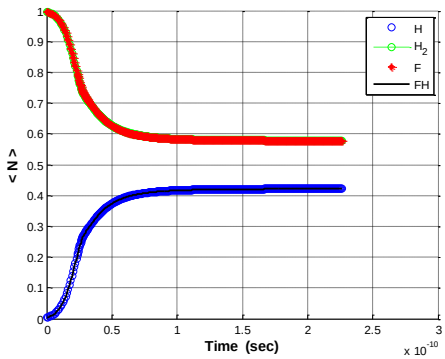

Figure 3. The expectation values of the particle number operator for each species.

A key feature of the IQT framework is that it is able to dynamically predict the concentration of reactive species as the reaction evolves in time. Figure 3 shows how the reactive species are depleted and created throughout the entire reaction process. Indeed the availability of these instantaneous values for the species concentrations indicates that the reaction rate constant $k(T)$, which in the literature is usually referred to as the thermal rate constant[1], may in fact not be a constant but rather a parameter changing in time. In Figure 3, the identical amounts for the reactants F and H_2 as well as for the products H and FH is a direct consequence of the proportionality relations, Eq. (5), and the initial amounts chosen for the reactants and products.

For the bimolecular reaction mechanism of Eq. (1), the net reaction rate as a function of time t is given by

$$r(t) = r_f(t) - r_b(t) \tag{34}$$

$$r(t) = k_f(t,T)[F(t)][H_2(t)] - k_b(t,T)[FH(t)][H(t)] \tag{35}$$

where r_f and r_b are the forward and backward reaction rates, k_f and k_b the forward and backward reaction rate "constants", and $[A(t)]$ the concentrations of the various species. The reaction orders for the species F, H_2, FH, and H coincide here with the stoichiometric coefficients for each species for this reaction mechanism although it is noted that this is not generally the case [23]. Based on the initial amounts of species chosen and the proportionality relations, it follows that the net reaction rate r for this reaction mechanism coincides with the expectation value of the rate of the reaction coordinate $\langle \dot{\varepsilon} \rangle$ given by Eq. (20). Numerically, it can also be found by calculating the slope of the expectation value of the particle number operator of either one of the product species using a second order accurate finite difference scheme. Once known, Eq. (35) along with the zero rate condition at stable equilibrium and the assumption that the detailed balance condition holds also for the time-dependent rate constants, i.e.,

$$\frac{k_f(t,T)}{k_b(t,T)} = \frac{k_f(t_{se},T)}{k_b(t_{se},T)} = \frac{[F]_{se}[H_2]_{se}}{[FH]_{se}[H]_{se}} \tag{36}$$

can be used to determine $k_f(t,T)$ and $k_b(t,T)$ at every instant of time along the entire kinetic path determined by the equation of motion.

Figure 4 shows these instantaneous values as well as the equilibrium constant $K(T)$ given by the ratio of k_f to k_b for the case of a system expectation energy which corresponds at stable equilibrium to a temperature of 298 K. The instantaneous values for the corresponding net, forward, and backward reaction rates are seen in Figure 5. Clearly, as expected, the forward reaction dominates at the beginning of the reaction with the reverse reaction growing in importance as stable equilibrium is approached. Note that the time scale seen in these two figures and the previous ones is based on a value of τ in the equation of motion which has been fitted to the value of k_f at 298 K reported in Heidner *et al.* [24] and shown in Table 2. This table also includes the values of k_f from Heidner *et al.* [24] for a number of other stable equilibrium temperatures as well as values for k_f from a number of other researchers.

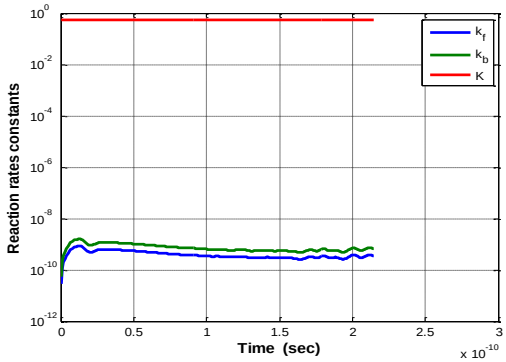

Figure 4. The forward and reverse reaction rate constants as well as the equilibrium constant as a function of time for a system expectation energy, which at stable equilibrium corresponds to a temperature of 298 K.

For a value of τ based on the value for k_f in Table 2 from Heidner *et al.* [24] corresponding to a stable equilibrium tem-

[1] In fact, this reaction rate constant is that for the forward reaction found at the start of the reaction when the backward reaction rate is negligible [22].

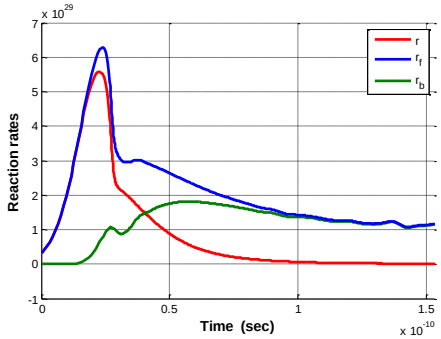

Figure 5. The forward, reverse and net reaction rates for a system expectation energy, which at stable equilibrium corresponds to a temperature of 298 K.

Table 2. Values of the forward reaction rate constant reported in the literature for the reaction mechanism of Eq. (1) [16].

k_f(T)/10^{-11} (cm^3/molecule-sec)					
T (K)	WH[a]	SBA[b]	HBGM[c]	RHPB[d]	WTM[e]
298	2.33	2.48	2.93	2.81	2.26
350	2.89	3.14	3.94	3.35	
400			4.88	3.80	
450			5.76		
500			6.57		
600			8.01		5.68
700			9.23		

[a]Wurzberg and Houston [25]; [b]Stevens, Brune, and Anderson [26]; [c]Heidner, Bott, Gardner, and Melzer [24]; [d]Rosenman, Hochman-Kowal, Persky, and Baer [27]; [e]Wang, Thompson and Miller [16]

perature of 700 K, a similar evolution of the reaction rate constants and reaction rates is given in Figures 6 and 7. The trends are the same as in Figures 4 and 5 with the forward reaction dominating initially and the backward reaction growing in importance as stable equilibrium is approached. However, the reaction rate magnitudes are clearly much greater and the difference between the forward and backward reaction rate constants is significantly larger.

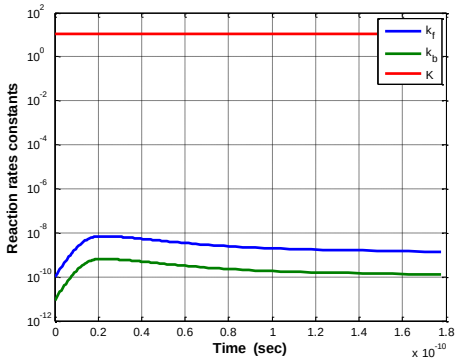

Figure 6. The forward and reverse reaction rate constants and the equilibrium constant as a function of time for a system expectation energy, which at stable equilibrium corresponds to a temperature of 700 K.

Although all the previous figures are referred to some stable equilibrium temperature, the use of such a temperature in the IQT simulations for the reaction kinetics of the reacting system is not required. What is required is a value for the system expectation energy. However, to make comparisons with the literature, this energy must be referred to its corresponding stable equilibrium temperature, i.e., the temperature at which a given reaction rate constant is reported in the literature (e.g., see Table 2). Thus, the temperatures indicated in Table 2 and in

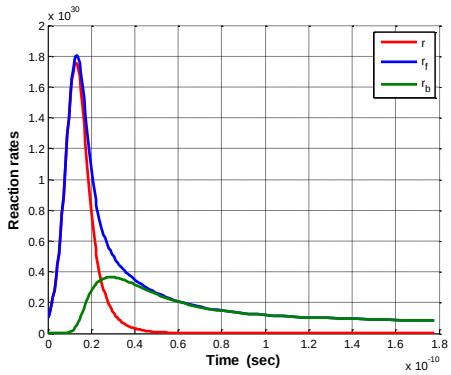

Figure 7. The forward, reverse and net reaction rates for a system expectation energy, which at stable equilibrium corresponds to a temperature of 700 K.

each of the figures are those calculated based on the stable equilibrium expression for the expectation energy of an ideal gas mixture obtained from the maximum entropy principle (MEP). These temperatures are based on a reactive system with an infinite number of degrees of freedom (DOF). Of course, in the IQT simulations, the non-equilibrium temperature θ_H (Eq. (23)) also converges to a given stable equilibrium temperature for each expectation energy. However, this temperature necessarily differs from that based on an infinite number of DOF since it is based on a finite number. For the reactive system considered here, a comparison of these temperatures is given in Table 3.

Table 3. IQT and MEP stable equilibrium temperature comparison.

T^{MEP} (K)	298	350	400	450	500	600	700
T^{IQT} (K)	121	284	427	565	704	1007	1364

SOME FURTHER RESULTS

A fundamental difference between the results for the reaction rate constant obtained by theories based on quantum mechanics to those based on classical mechanics is the divergence from linear behaviour at low temperatures as illustrated in Figure 8. For the system considered here and within the IQT framework, Figure 9 shows the behaviour of the forward reaction rate constant as a function of stable equilibrium temperature (T^{MEP}). Clearly, the deviation from linear behaviour at low temperatures seen in this figure provides confirmation that the predictions being made with IQT follow what would be expected from a quantum mechanically based model. Of course, additional validation of the IQT predictions is needed. In principle, it would be interesting to see if it is possible to identify a fixed, physically meaningful functional $\tau(\rho)$ such that (1) $k_f(t,T)$ and $k_b(t,T)$

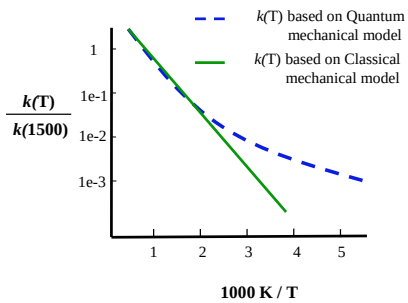

Figure 8. Depiction of the temperature dependence of the forward reaction rate constant with and without quantum mechanical effects taken into account.

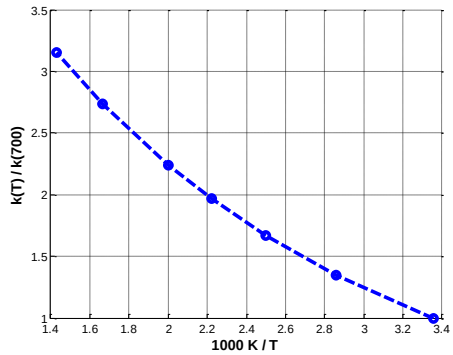

Figure 9. Temperature (T^{MEP}) dependence of the forward reaction rate constant for various stable equilibrium temperatures.

as computed above from the assumption of the detailed balance result are effectively independent of time and (2) the reaction rates match the data of Table 2 without the need for adjusting any parameter. This validation has not yet been done. Instead the values used for τ are those, as mentioned earlier, which simply fit the values in column four of Table 2. Figure 10 is a plot of these values as a function of stable equilibrium temperature (T^{MEP}). The authors are presently working on a functional for τ, and Figure 10 provides a basis for understanding at least some part of the behaviour, which such a functional must reflect. Knowing the expected behaviour of τ should help in identifying a unique functional $\tau(\rho)$ capable of capturing the dynamics of the reaction without the use of adjustable parameters.

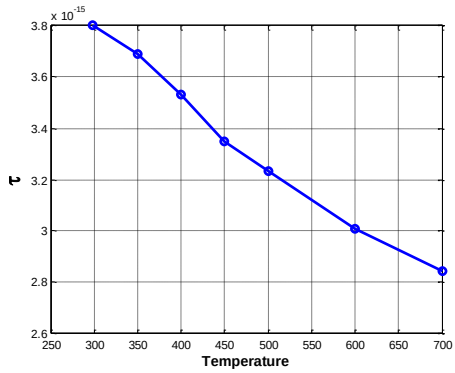

Figure 10. Relaxation time constant for the various stable equilibrium temperatures (T^{MEP}) found in Table 2.

CONCLUSIONS

The IQT framework provides a comprehensive and reasonable approach for predicting the chemical kinetics of small scale reactive systems that could become a valid alternative to conventional approaches. Because IQT unifies quantum mechanics and thermodynamics into a single theory with a single internally consistent kinematics and dynamics, the laws of both are automatically satisfied when modeling reactive or non-reactive systems at the atomistic level. The consequence is that unlike conventional methods that use hybrid approaches to try to predict details of the kinetics of a change in state, IQT holds the promise to provide a full set of thermodynamically consistent, time-dependent features of the chemical kinetics of an atomistic-scale, chemically reactive system.

Finally, the preliminary data presented in this paper demonstrates that the predictions of IQT appear consistent with what the best conventional methods in the literature are able to predict. For very few particle systems and by considering a small set of energy levels the computational burden is not large at all.

ACKNOWLEDGMENTS

The second author gratefully acknowledges the Cariplo-UniBS-MIT-MechE faculty exchange program co-sponsored by UniBS and the CARIPLO Foundation, Italy, under grant 2008-2290, EOARD (European Office of Aerospace R&D) grant FA8655-11-1-3068, and Italian MIUR grant PRIN-2009-3JPM5Z-002.

REFERENCES

[1] Hatsopoulos, G. N. and Gyftopoulos, E. P., *Foundations of Physics,* **6**(1), 15-31, 1976.
[2] Hatsopoulos, G. N. and Gyftopoulos, E. P., *Foundations of Physics,* **6**(2), 127-141, 1976.
[3] Hatsopoulos, G. N. and Gyftopoulos, E. P., *Foundations of Physics,* **6**(4), 439-455, 1976.
[4] Hatsopoulos, G. N. and Gyftopoulos, E. P., *Foundations of Physics,* **6**(5), 561-570, 1976.
[5] Beretta, G. P., *On the general equation of motion of Quantum Thermodynamics and the distinction between quantal and nonquantal uncertainties*, Sc.D. dissertation, (advisor: E. P. Gyftopoulos, MIT, Cambridge, MA), 1981.
[6] Beretta, G. P., Gyftopoulos, E. P., Park, J. L., Hatsopoulos, G. N., *Il Nuovo Cimento B*, **82**, 169-191, 1984.
[7] Beretta, G. P., Gyftopoulos, E. P., and Park, J. L., *Nuovo Cimento B*, **87**, 77, 1985.
[8] Beretta, G. P., *Rep. on Math. Phys.,* **64**(1), 139-168, 2009.
[9] Beretta, G. P., *J. Phys.: Conf. Ser.* **237**, 012004, 2010.
[10] Smith, C. E., *Intrinsic Quantum Thermodynamics: Application to Hydrogen Storage on a Carbon Nanotube and Theoretical Consideration of Non-Work Interactions*, (advisor: M. R. von Spakovsky, Virginia Tech), 2012.
[11] Laidler, K. J. and King, M. C., *Journal of Physical Chemistry,* **87**(15), 2657-2664, 1983.
[12] Truhlar, D. G., Garrett, B. C., Klippenstein, S. J., *Journal of Physical Chemistry,* **100**(31), 12771-12800, 1996.
[13] Aoiz, F. J., Bañares, L., Díez-Rojo, T., Herrero, V. J., Sáez Rábanos, V., *J. of Phys. Chem.,* **100**(10), 4071-4083, 1996.
[14] Schatz, G. C., *Journal of Physical Chemistry,* **100**(31), 12839-12847, 1996.
[15] Althorpe, S. C. and Clary, D. C., *Annual Review of Physical Chemistry,* **54**(1), 493-529, 2003.
[16] Wang, H., Thompson, W. H. and Miller, W. H. *Journal of Physical Chemistry A,* **102**(47), 9372-9379, 1998.
[17] Aquilanti, V., Cavalli, S., De Fazio, D., Volpi, A., Aguilar, A., Lucas, J. M., *Chem. Phys.,* **308**(3), 237-253, 2005.
[18] Beretta G. P. and von Spakovsky, M. R., in preparation.
[19] Ziegler, H., *J of Appl. Math. and Phys.* (ZAMP) **34** 832-844, 1983.
[20] Gyftopolous, E. P., Beretta, G. P., *Thermodynamics: Foundations and Applications,* 2nd ed. (NY: Dover), 2005.
[21] Borysow, A., *Astr. and Astrophys.*, **390**(2), 779-782, 2002.
[22] Levine, R. D., *Molecular Reaction Dynamics*, Cambridge University Press, N.Y., 2005.
[23] Carr, R. W., Modeling of Chem. Reactions, Elsevier, 2007.
[24] Heidner, R. F., Bott, J. F., Gardner, C. E., Melzer, J. E., *The Journal of Chemical Physics*, **72**(9), 4815-4821, 1980.
[25] Wurzberg, E. and Houston, P. L., *The Journal of Chemical Physics*, **72**(9), 4811-4814, 1980.
[26] Stevens, P. S., Brune, W. H. and Anderson, J. G., *The Journal of physical chemistry*, **93**(10), 4068-4079, 1989.
[27] Rosenman, E., Hochman-Kowal, S., Persky, A. and Baer, M., *Chemical Physics Letters*, **257**(5–6), 421-428, 1996.